

Analyst

Accepted Manuscript



This is an *Accepted Manuscript*, which has been through the Royal Society of Chemistry peer review process and has been accepted for publication.

Accepted Manuscripts are published online shortly after acceptance, before technical editing, formatting and proof reading. Using this free service, authors can make their results available to the community, in citable form, before we publish the edited article. We will replace this *Accepted Manuscript* with the edited and formatted *Advance Article* as soon as it is available.

You can find more information about *Accepted Manuscripts* in the [Information for Authors](#).

Please note that technical editing may introduce minor changes to the text and/or graphics, which may alter content. The journal's standard [Terms & Conditions](#) and the [Ethical guidelines](#) still apply. In no event shall the Royal Society of Chemistry be held responsible for any errors or omissions in this *Accepted Manuscript* or any consequences arising from the use of any information it contains.

1
2
3 Highly Sensitive Electrochemical Detection of DNA Hybridisation by
4
5
6 Coupling the Chemical Reduction of a Redox Label to the Electrode
7
8
9 Reaction of a Solution Phase Mediator
10
11
12

13 Umphan Ngoensawat¹, Patsamon Rijiravanich², Mithran Somasundrum², Werasak
14
15 Surareungchai^{1,3}
16
17
18
19
20
21

22 ¹*School of Bioresources and Technology, King Mongkut's University of Technology*
23 *Thonburi, Bang Khun Thian, Bangkok 10150, Thailand*
24

25 ²*Biochemical Engineering and Pilot Plant Research and Development Unit, National*
26 *Center for Genetic Engineering and Biotechnology, National Science and Technology*
27 *Development Agency at King Mongkut's University of Technology Thonburi, Bang*
28 *Khun Thian, Bangkok 10150, Thailand*
29

30 ³*Biological Engineering Graduate Program, King Mongkut's University of*
31 *Technology Thonburi, Bangmod, Bangkok 10140, Thailand*
32
33
34
35
36
37
38

39 *Authors for correspondence: mithran.somasundrum@gmail.com,
40 werasak.sur@kmutt.ac.th
41
42
43
44
45
46
47
48
49
50
51
52
53
54
55
56
57
58
59
60

ABSTRACT

We have described a highly sensitive method for detecting DNA hybridisation, using a redox-labeled stem loop probe. The redox labels were poly(styrene-co-acrylic) (PSA) spheres of 454 nm diameter, modified by methylene blue (MB) deposited alternatively with poly(sodium 4-styrene sulphonate) (PSS) in a layer-by-layer process. Each PSA sphere carried approx. 3.7×10^5 molecules of MB, as determined optically. DIG-tagged stem loop probes were immobilised on screen printed electrodes bearing anti-DIG antibodies. Binding with target enabled straightening of the stem loop, which made attachment to the MB-coated PSA spheres possible. Measuring the current from the direct reduction of MB by differential pulse voltammetry, a 30 mer DNA target common to 70 strains of *Escherichia coli* was calibrated across the range 1.0 fM to 100 pM (gradient = 3.2×10^{-8} A (log fM)⁻¹, $r^2 = 0.95$, $n = 60$), with an LOD of ~ 58 fM. By using Fe(CN)₆^{3-/4-} as a solution phase mediator for the MB reduction, we were able to lower the LOD to ~ 39 aM (gradient = 5.95×10^8 A (log aM)⁻¹, $r^2 = 0.96$, $n = 30$), which corresponds to the detection of 0.76 ag (~ 50 molecules) in the 2 µL analyte sample. We hypothesise that the lowering of the LOD was due to the fact that not all the MB labels were able to contact the electrode surface.

Keywords: Stem loop; differential pulse voltammetry; mediator; E. coli; layer-by-layer.

1. Introduction

There is currently great interest in sequence-specific DNA detection, due to potential for application in gene analysis, clinical diagnosis, forensic and environmental science and monitoring food safety.¹⁻⁵ Of the different detection methods available, electrochemistry has been intensively researched, due to the fact that electrochemical reactions produce an electrical signal without needing expensive transduction equipment, while having the potential for on-site, decentralized testing, and can be coupled with current minaturization technologies. To achieve sufficiently low detection limits with electrochemical systems, a number of different strategies have been attempted. DNA sequences have been amplified by enzymatic means, such as the polymerase chain reaction (PCR).⁶ While this technique significantly lowers the detection limit, it increases the number of assay steps and therefore assay time, and requires both expensive equipment and trained personnel. Other enzymatic methods have involved nuclease enzymes,^{7,8} but these still require adding further steps to the assay.

If measurement is to be performed without sequence amplification, then the means of detecting hybridisation itself must be sensitive enough for the given application. Although label-free methods have been proposed,⁹⁻¹¹ generally speaking, detection via electrochemical labels has provided better sensitivities. Enzyme labels¹² have enabled very low detection limits but can suffer the problem of instability due to loss of enzyme activity over time. The alternative is to either use a nanometal or a redox label. Both require a reporter probe orientation such that the label is in contact with the electrode surface. In the nanometal case, if contact is not complete, the metal in question can still be measured by anodic stripping voltammetry, following acid dissolution.¹³ However, this introduces further measurement steps. A redox molecule

1
2
3 can either be intercalated in the ssDNA or dsDNA structure,^{14,15} or tagged to the end
4
5 of the sequence. Intercalation means that the amount of redox charge delivered per
6
7 DNA strand can only be increased by increasing the length of the strand. Where as in
8
9 the case of an end-tagged DNA sequence, the quantity of charge delivered for a given
10
11 sequence length can be increased by rational design of the redox label. Examples of
12
13 DNA probes tagged with individual redox molecules include ferrocene attached to
14
15 amino-modified DNA probes at one end,¹⁶ and methylene blue (MB) attached to
16
17 DNA probes at one or both ends.¹⁷ Strategies to increase the number of redox
18
19 molecules delivered per hybridisation event include: four ferrocene molecules bound
20
21 linearly to a stem loop probe,¹⁸ Ru(NH₃)₆³⁺ molecules contained in a liposome label¹⁹
22
23 and carbon nanotubes loaded with tris(2,2'-bipyridyl) ruthenium derivatives.²⁰ All of
24
25 the aforementioned methods employed direct reaction of the mediator at the electrode
26
27 surface. This may not always be the best strategy. Increasing the number of redox
28
29 units per DNA probe will inevitably mean increasing the surface area/volume of the
30
31 solid support. This raises the question of whether all redox molecules on the support
32
33 can have adequate contact with the electrode surface. A further problem may arise
34
35 from steric hindrance between neighbouring probes preventing a probe label actually
36
37 reaching the electrode surface. A way to avoid these inefficiencies would be to use a
38
39 second redox couple in solution, to mediate electron transfer from the label-bound
40
41 species. To the best of our knowledge, this strategy has not so far been examined.
42
43 Hence, in this work we describe the construction of electrochemical labels bearing a
44
45 high quantity of redox molecules (sub-micron size latex particles loaded with MB by
46
47 layer-by-layer deposition). We used these labels to tag stem loop probes containing a
48
49 30 mer sequence common to 71 strains of *E. coli*. We show how a) the high quantity
50
51 of MB provided a low detection limit and b) by mediating electron transfer from the
52
53
54
55
56
57
58
59
60

1
2
3 MB using a solution phase redox couple ($\text{Fe}(\text{CN})_6^{3-/4-}$) we could lower that detection
4
5 limit even further.
6
7
8
9
10

11 12 13 14 **2. Experimental**

15 16 *2.1 Apparatus*

17
18 UV-visible spectra were recorded using a Schott UV-Vis spectrometer model Uvikon
19
20 XL. Electrochemical experiments were performed using an Autolab PGSTAT 10
21
22 computer-controlled potentiostat (Eco Chemie) with GPES software. Screen-printed
23
24 electrodes (SPEs) were fabricated in-house exactly as described previously²¹ and
25
26 possessed a 1.5 mm × 3.5 mm carbon track working electrode and a 2 mm × 3.5 mm
27
28 Ag/AgCl track combined reference/counter electrode.
29
30
31
32
33
34
35

36 37 *2.2 Reagents and solutions*

38
39 Anti-Digoxigenin (Anti-DIG) was purchased from Genway. The synthetic
40
41 oligonucleotides were purchased from Thermoscience. Oligonucleotide stock
42
43 solutions (100 μM) were prepared with sterile milliQ water and kept frozen. The
44
45 probe and target oligonucleotides solutions were diluted using 10 mM phosphate
46
47 buffer, pH 7.0, containing 0.1 M NaCl. Poly(allylamine hydrochloride) (PAA)
48
49 (molecular weight ≈ 70000 g mol⁻¹), poly(sodium 4-styrene-sulfonate) (PSS)
50
51 (molecular weight ≈ 70000 g mol⁻¹), tween 20, poly-L-lysine (PLL) and avidin were
52
53 purchased from Sigma-Aldrich. MilliQ water was used for all the solution
54
55 preparations.
56
57
58
59
60

The DNA strands had the following sequences:

Stem loop probe: anti-DIG-5'-AAA GGC CGT CTT CCT GAG TAA TAA CTT

CCT GAG TGA ATA ACG GCC AAA AA-3'-biotin

30 mer Target DNA: 5'-TAT TCA CTC AGG AAG TTA TTA CTC AGG AAG-3'

20 mer Target DNA: 5'- GGA AGT TAT TAC TCA GGA AG -3'

1 Mismatch DNA: 5'-TAT TCA CTC AGC AAG TTA TTA CTC AGG AAG-3'

3 Mismatch DNA: 5'-TAT TCA CTC AGC AAC TTA TTA CTC ACG AAG-3'

30 mer noncomplementary DNA: 5'-TCA TTT AGC TTT GTT AGC GTT AGG
TAT ATC-3'

50 mer-noncomplementary DNA: 5'-AGT AAT GGA ACG GTT GCT CTT CAT
TTA GCT TTG TTA GCG TTA GGT ATA TC-3'

2.3 Preparation of MB-Ball label

PSA particles were synthesised by reacting together styrene and acrylic acid in a nitrogen-purged aqueous solution in the presence of ammonium persulphate. The polymerisation time was 8 h. Full details are given in Pinijsuwan et al.²¹ A suspension of 90.5 mg of PSA particles was sonicated in 10 mL of 95% ethanol until well dispersed. The ethanol was then removed after by centrifugation at 10,000 rpm for 15 min and the particles redispersed in 10 mL of milliQ water. After that the PSA particles were sequentially incubated in 20 mL of PAA, PSS, PAA and PSS solutions (1 mg mL⁻¹ in 0.5 M NaCl). Each polyelectrolyte layer was allowed to adsorb for 30 min at room temperature, and then three centrifugations/redispersions steps were performed with sterile milliQ water before incubation in the next solution. The

1
2
3 polyelectrolyte-coated PSA spheres (PSA-PE₄) were stored in 20 mL of milliQ water
4
5 (approx. PSA concentration = 42.27 mg mL⁻¹) at room temperature.
6

7
8 Methylene blue-loaded latex particles (MB-Ball) were prepared by adding 8
9
10 mL of 1 mM methylene blue to a 20 mL dispersion of 2.5 mg mL⁻¹ PSA-PE₄ particles.
11
12 The mixture was incubated for 30 min under stirring at room temperature and then
13
14 triplicate centrifugation and redispersion cycles were performed using 8 mL of milliQ
15
16 water, to remove unadsorbed methylene blue. Following this the PSA-PE₄ particles
17
18 were incubated in a 20 mL solution of 0.5 M NaCl containing 1 mg mL⁻¹ of PSS for
19
20 30min. These steps were repeated to give 3 layers of methylene blue on the PSA-PE₄.
21
22 Finally the MB-ball particles were dispersed in 20 mL of sterile milliQ water at a
23
24 concentration of approx. = 3.3 mg mL⁻¹.
25
26
27
28
29
30
31
32
33

34 *2.4 Preparation of MB-Ball/Avidin Conjugate*

35
36 A 1 ml suspension of MB-Ball particles was centrifuged and then redispersed in 990
37
38 μ L of 10 mM phosphate buffer, pH 7.0, containing 0.1 M NaCl. A 10 μ L aliquot of
39
40 avidin solution (21.14 mg mL⁻¹) was then added and the mixture was incubated under
41
42 stirring at room temperature for 90 min. After that the solution was centrifuged and
43
44 washed three times with 10 mM phosphate buffer, pH 7.0, containing 0.1 M NaCl, to
45
46 remove any free avidin. The MB-ball/avidin was stored in sterile 10 mM phosphate
47
48 buffer, pH 7.0, at 4 °C prior to use.
49
50
51
52
53
54
55
56
57
58
59
60

1
2
3 *2.5 Preparation of anti-Digoxigenin (anti-DIG) modified screen-printed electrode*
4
5 *(SPE)*
6

7 The SPE was washed with sterilized Milli-Q water and then dried under a nitrogen
8 stream before use. A 10 μ L aliquot of poly-L-lysine (PLL) was deposited on the
9 working area and incubated at room temperature for 20 min. The electrodes were
10 then dried at 80 °C for 10 min, followed by dipping in 5 mL 10 mM phosphate buffer,
11 pH 7.0, containing 0.1 M NaCl, and then drying under nitrogen. The SPE surface was
12 then exposed to a 5 μ L aliquot of between 5 to 98 μ g mL⁻¹ of anti-DIG in 0.1 M
13 phosphate buffer, pH 7.0, containing 1.0 M NaCl. The anti-DIG molecules were
14 allowed to adsorb for 30 min at 25 °C, following which the SPE was rinsed twice
15 (approx. 1 mL each rinse) with sterilized 10 mM phosphate buffer containing 0.1 M
16 NaCl + 0.5% tween, then rinsed five times with the same buffer/electrolyte
17 combination in the absence of tween, and then dried under nitrogen.
18
19
20
21
22
23
24
25
26
27
28
29
30
31
32
33
34
35
36
37

38 *2.6 Detection of DNA hybridization using MB-Ball labels based on stem loop probe*
39

40 Into each PCR tube were deposited 20 μ L of 1 μ M stem-loop DNA probe, 20 μ L of
41 target DNA and 60 μ L 100 mM phosphate buffer, pH 7.0 + 1.0 M NaCl. The tube
42 was incubated for 60 min, at 45 °C unless otherwise stated. A 10 μ L aliquot was then
43 removed from the tube and deposited on the surface of the SPE to allow binding
44 between the surface-confined anti-DIG and DIG-tagged stem-loop DNA probe. The
45 SPE was then rinsed twice with 10 mM phosphate buffer + 0.1 M NaCl + 0.5 %
46 tween, and five times with 10 mM phosphate buffer, pH 7.0 + 0.1 M NaCl, both
47 buffers being at 4 °C. The SPE was then dried under a nitrogen stream. The MB-
48
49
50
51
52
53
54
55
56
57
58
59
60

1
2
3 Ball/avidin suspension prepared as described in section 2.3 was diluted in a 1:1 ratio
4
5 with 0.1 M phosphate buffer, pH 7.0, containing 1.0 M NaCl. This was used as the
6
7 labeling solution. A 5 μ L aliquot of this solution was deposited on the SPE, which
8
9 was then left to stand for 30 min on a temperature-controlled mixing block (Bioer,
10
11 model MB-102) set to 15 $^{\circ}$ C. This was followed by rinsing twice with 10 mM
12
13 phosphate buffer + 0.1 M NaCl + 0.5 % tween, and five times with 10 mM phosphate
14
15 buffer, pH 7.0 + 0.1 M NaCl, both solutions used at 4 $^{\circ}$ C. The SPE was then dried
16
17 under a nitrogen stream. A 50 μ L aliquot of 0.1 M phosphate buffer, pH 7.0 + 1.0 M
18
19 NaCl (containing 0.25 mM potassium ferricyanide when mediated electron transfer
20
21 was implemented) was then deposited over both electrodes (carbon working electrode
22
23 and Ag/AgCl combined reference and counter). Differential pulse voltammetry
24
25 (DPV) was performed using the conditions: step potential = 72 mV, amplitude = 50
26
27 mV, scan rate = 5 mV s⁻¹.
28
29
30
31
32
33
34
35
36
37
38
39
40

41 **3. Results and Discussion**

42 *3.1 Construction of Redox Labels*

43
44
45 Based on TEM measurement, the PSA spheres had a mean diameter of 454 nm and a
46
47 relatively narrow size distribution (1 std. dev. = 3.0 nm, $n = 100$ particles). The PSA
48
49 spheres possess a negative surface charge excess at neutral pH, due to deprotonation of
50
51 the acid groups.²² We used this fact to coat the spheres with two oppositely charged
52
53 polyelectrolyte bilayers, i.e. (PAA/PSS)₂, in a layer-by-layer (l-b-l) process as
54
55
56
57
58
59
60

1
2
3 described previously.²¹ TEM measurement of the coated spheres indicated an
4 increase in diameter to 461 nm (1 std. dev. = 2.6 nm, $n = 100$ particles). The main
5 driving force for l-b-l deposition is electrostatic attraction, due to the fact that charge
6 overcompensation occurs with the deposition of each layer, causing the zeta potential
7 to oscillate symmetrically between positive and negative values.²³ Hence, the
8 (PAA/PSS)₂ coating is expected to present an overall negative surface charge to the
9 solution. Contributing factors to l-b-l deposition include Van der Waals forces,
10 hydrogen bonding and hydrophobic interactions, as well as an increase in entropy due
11 to the liberation of counter ions and solvent shell water molecules. For this reason, it
12 has been found possible to replace one of the l-b-l polyelectrolytes with a smaller
13 charged species, such as Eu³⁺.²⁴ This allowed us to l-b-l deposit the positively
14 charged redox molecule methylene blue (MB) between layers of negatively charged
15 PSS. The completed structure was PSA-(PAA/PSS)₂(MB/PSS)₃. Building up the MB
16 layers caused the PSA spheres to change from white to blue (see Supporting
17 Information, Fig. S-1). The quantity of MB loaded was determined by dissolving the
18 PSA in tetrahydrofuran (THF) and measuring the absorbance of the solution. As
19 shown in Fig. 1, the absorbance spectra of a solution of dissolved spheres (peak at 622
20 nm, shoulder at 614 nm) was consistent with the spectra of pure MB in MilliQ water.
21 Using the peak at 662 nm to plot a linear calibration curve ($Abs_{622\text{ nm}} = 0.0078c$ (μM)
22 - 0.0083, $r^2 = 0.9993$, $n = 11$), we determined the molar extinction coefficient of MB
23 in THF to be $7.6 \times 10^3 \text{ M}^{-1} \text{ cm}^{-1}$. Based on the TEM radius we determined the mass
24 of one PSA sphere to be $5.15 \times 10^{-14} \text{ g}$, assuming a density of 1.05 g cm^{-3} .²⁵ The dry
25 weight of an aliquot of known volume was then used to calculate the concentration of
26 particles in the suspension, which was found to be 2.8×10^{10} PSA-
27 (PAA/PSS)₂(MB/PSS)₃ particles mL⁻¹. Based on this concentration, the absorbance
28
29
30
31
32
33
34
35
36
37
38
39
40
41
42
43
44
45
46
47
48
49
50
51
52
53
54
55
56
57
58
59
60

1
2
3 from the dissolution of a known aliquot corresponded to a loading of 3.7×10^5 MB
4 molecules per PSA sphere.
5
6
7
8
9

10 11 12 13 14 *3.2 Detection of DNA Hybridisation by Direct Methylene Blue Reaction*

15
16 The principle of hybridisation detection using redox-labelled stem loop DNA is
17 illustrated in Scheme 1. The detection concept is based on the following sequence: 1)
18 Homogeneous hybridisation between DIG-tagged stem loop probe and DNA target.
19 2) Binding of the DIG tag to electrode-confined anti-DIG antibodies. 3) Exposure of
20 the immobilised DNA to cold buffer solution (~ 4 °C). Since this temperature is
21 below the melting temperature, T_m , of the stem loop sequence (T_m stem loop = 30.87
22 °C (www.rnasoft.ca)) the stem loop reforms in the DNA strands that are not bound to
23 target. Where probe-target binding occurs, the duplex remains unaffected due to
24 probe-target formation possessing a more negative free energy than stem loop
25 formation (T_m target-probe = 73.36 °C.²⁶ 4) Attachment between biotin tag at the 3'
26 end of the hybridised probes and the avidin coating of the PSA-
27 (PAA/PSS)₂(MB/PSS)₃ spheres. The unhybridised probes do not form the avidin-
28 biotin bond due to the stem loop causing steric hindrance to the approach of the
29 relatively large PSA labels. 5) Voltammetric detection of the PSA-
30 (PAA/PSS)₂(MB/PSS)₃ labels through either direct reduction or redox mediation
31 using solution phase $\text{Fe}(\text{CN}_6)^{4-}$.
32
33
34
35
36
37
38
39
40
41
42
43
44
45
46
47
48
49
50
51
52
53
54
55
56
57
58
59
60

3.3 Optimisation of DNA Hybridisation Detection

Immobilisation of the anti-DIG antibodies on screen printed electrodes was performed by first coating the electrodes with poly-L-lysine, following the observation that antibodies can be stably bound to this surface and can retain the ability to capture their relevant antigens.²⁷ Since poly-L-lysine is positively charged, we expect the binding mechanism to be electrostatic. The concentration of anti-DIG exposed to the coated electrodes was varied in the range 5 to 98 $\mu\text{g mL}^{-1}$ and the differential pulse voltammetric (DPV) peak height from direct MB reduction was recorded in the absence of target DNA (I_0) and in the presence of 1 pM of target DNA (I). Five electrodes were examined at each anti-DIG concentration. The result is shown in Fig. 2. It can be seen that the I/I_0 ratio reaches a maximum value at an immobilising solution concentration of 19.9 $\mu\text{g mL}^{-1}$ and then decreases. We expect this is because a) at highly dense probe coverages steric hindrance lowers the efficiency of PSA(PAA/PSS)₂(MB/PSS)₃ attachment to the DNA probe, b) high density coverages may prevent horizontal alignment of DNA duplexes at the electrode surface. Such alignment is necessary for MB-electrode contact.

Using the 19.9 $\mu\text{g mL}^{-1}$ stock for anti-DIG immobilisation we varied the hybridisation temperature from 30 °C to 60 °C. The effect of this on the previously defined I/I_0 ratio is shown in Fig. 3. It can be seen the optimum hybridisation temperature was 45 °C. As noted earlier, T_m of the probe-target duplex, (defined as the temperature where half the dsDNA in the sample is dehybridised) was calculated to be 73.36 °C. Hence, the optimum temperature found here is consistent with the general rule of thumb that the optimum hybridisation temperature is approx. 20 - 25 °C below T_m .²⁸

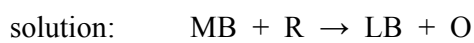
3.4 Specificity and Sensitivity Utilising Direct MB Reduction

Under the optimised conditions for hybridisation detection using direct MB reduction, we examined the assay specificity as follows: The responses to 1 pM and 100 fM of complementary target (30 mer) were compared to the responses for (a) 1 pM of a 50 mer non-complementary target, (b) 1 pM of a 30 mer non-complementary target, (c) 100 fM of a 30 mer one base mismatch, (d) 100 fM of a three base mismatch. Five electrodes were used for each target. As shown in Fig. 4, the 50 mer non-complementary target produced a negligible response, while the 30 mer non-complementary target, one base and three base mismatches produced responses significantly lower ($\sim 25\%$) than the complementary strands. Based on a suggestion by one of the reviewers, we performed comparative assays on a one base mismatched target (100 fM) in which the washing of the screen printed electrode after target binding was performed a) using 10 mM phosphate buffer, pH 7.0 + 0.1 M KCl, as described in the Experimental section, and b) first using the same washing buffer at 45 °C prior to washing with the buffer at 0 °C. We found that washing with the buffer at 45 °C lowered the value of I/I_0 to almost zero for the one base mismatch, while a response to 100 fM complementary target could still be realised (see Supporting Information, Fig. S-2). It is likely that some probe-mismatch target opening occurred at the higher temperature. Fig. 5 shows a calibration of the complementary target under the optimised assay conditions, plotted on a log scale. It can be seen that the response was linear with the logarithm of concentration in the range 1.0 fM to 100 pM (gradient = 3.2×10^{-8} A (log fM) $^{-1}$, $r^2 = 0.95$, $n = 60$). We apply the commonly accepted definition of limit of detection (LOD) as being the concentration giving a response equal to $\bar{x} + 3\sigma$, where \bar{x} is the mean response to a blank and σ is the standard deviation of that response.²⁹ Using the peak height to a 30 mer non-complementary

1
2
3 sequence as the blank, eight electrodes gave $\bar{x} = 1.30 \times 10^{-7}$ A, $\sigma = 6.52 \times 10^{-9}$ A, from
4
5 which LOD ~ 58 fM. For the 2 μ L aliquot dropped onto the electrode, this
6
7 corresponds to the detection of 1.07 fg or 0.12 amol, i.e. $\sim 7 \times 10^4$ DNA molecules.
8
9 This detection limit could be lowered further as described below.
10
11
12
13
14
15
16
17
18
19

20 *3.5 Sensitivity Enhancement Using a Solution Phase Mediator*

21 As noted earlier, realisation of a voltammetric current from the PSA-
22 (PAA/PSS)₂(MB/PSS)₃ label requires the DNA duplex to be essentially horizontal on
23 the electrode surface, since the MB must be close enough to the electrode for electron
24 transfer to occur. Given the large probability of steric hindrance from adjoining
25 duplexes, it is likely that not all the MB labels will make adequate surface contact. A
26 further consideration is whether charge percolation through the MB film is sufficient
27 for all the redox charge in the (MB/PSS)₃ coating to be transported to the electrode.
28
29 A method to circumvent these problems is to utilise redox cycling of the form:
30
31
32
33
34
35
36
37
38
39
40
41
42
43
44
45
46
47
48
49
50
51
52
53
54
55
56
57
58
59
60



Ostanta et al.³⁰ have detected DNA amination using the reactant system MB +
Fe(CN)₆³⁻. They showed that DPV peaks for Fe(CN)₆³⁻ reduction increased in the
presence of MB. Since both reactants are initially present in the oxidised form, the
explanation must be that within the timescale of the voltammetric reduction peak the
electrogenerated Fe(CN)₆⁴⁻ is converted back to Fe(CN)₆³⁻ by MB, thus raising the
concentration of Fe(CN)₆³⁻ at the electrode. We previously presented hydrodynamic

1
2
3 linear sweep voltammograms in support of this interpretation, and used $\text{Fe}(\text{CN})_6^{3-}$ to
4 mediate the reduction of MB adsorbed onto carbon nanotubes, for an immunoassay
5 label.³¹ Here we examined the use of $\text{Fe}(\text{CN})_6^{3-/4-}$ to mediate charge from the PSA-
6
7
8
9
10
11
12
13
14
15
16
17
18
19
20
21
22
23
24
25
26
27
28
29
30
31
32
33
34
35
36
37
38
39
40
41
42
43
44
45
46
47
48
49
50
51
52
53
54
55
56
57
58
59
60

linear sweep voltammograms in support of this interpretation, and used $\text{Fe}(\text{CN})_6^{3-}$ to mediate the reduction of MB adsorbed onto carbon nanotubes, for an immunoassay label.³¹ Here we examined the use of $\text{Fe}(\text{CN})_6^{3-/4-}$ to mediate charge from the PSA-(PAA/PSS)₂(MB/PSS)₃ spheres. We measured the direct and $\text{Fe}(\text{CN})_6^{3-/4-}$ - mediated reduction current in the absence of target DNA (I_0) and the presence of 1.0 pM of complementary target (I), while varying the quantity of $\text{Fe}(\text{CN})_6^{3-}$. The inset to Fig. 6 shows the values of I/I_0 as determined from both direct and redox-mediated reduction, as a function of $\text{Fe}(\text{CN})_6^{3-/4-}$ concentration. It can be seen that the I/I_0 ratio initially increased with mediator concentration, which can be attributed to the corresponding increase in the MB - $\text{Fe}(\text{CN})_6^{3-}$ reaction rate. At very high $\text{Fe}(\text{CN})_6^{3-}$ concentrations only a small proportion of the total $\text{Fe}(\text{CN})_6^{3-}$ is turned over by the MB, and therefore the peak height eventually decreases. As seen in the inset to Fig. 6, the optimum $\text{Fe}(\text{CN})_6^{3-}$ concentration was 0.25 mM. The main section of Fig. 6 shows the DPV recorded to 1.0 pM of target sequence, following hybridisation with the stem loop, in the absence and presence of 0.25 mM $\text{Fe}(\text{CN})_6^{3-/4-}$. We used this mediator concentration to calibrate target DNA across the range 0.1 fM to 25 fM as shown in Fig. 7 (gradient = 5.95×10^{-8} A (log aM)⁻¹, $r^2 = 0.96$, $n = 30$). Eight determinations of a 30 mer non-complementary sequence produced $\bar{x} = 4.46 \times 10^{-8}$ A, $\sigma = 7.59 \times 10^{-9}$ A. Applying the definition stated earlier produces LOD ~ 39 aM. For the 2 μL hybridisation solution this corresponds to the detection of ~ 0.72 ag or 0.1 zmol, i.e. ~ 50 DNA molecules. This is not as low as the LOD reported by Ferapontova et al.³² who used a lipase label to cleave ferrocene derivatives bound to an electrode (20 aM). However, to the best of our knowledge it is the lowest reported LOD for a redox label used on its own, without the presence of an enzyme. It is also lower than some recent reports of chemiluminescent hybridisation detection.^{33,34} For a given concentration of

1
2
3 target (100 fM) we noted some difference in the response to 20 mer and 30 mer
4
5 targets using both direct and mediated detection (direct detection: \bar{x} 20 mer = $2.85 \times$
6
7 10^{-8} A, $\sigma = 1.94 \times 10^{-9}$ A, \bar{x} 30 mer = 3.81×10^{-8} A, $\sigma = 9.68 \times 10^{-9}$ A, i.e. 25 %
8
9 difference. Mediated detection: \bar{x} 20 mer = 1.19×10^{-6} A, $\sigma = 8.21 \times 10^{-8}$ A, \bar{x} 30 mer
10
11 = 1.11×10^{-6} A, $\sigma = 1.00 \times 10^{-7}$ A, i.e. 8 % difference. $n = 5$ for all determinations).
12
13 Hence, although the use of mediated detection lowers the effect of target length, we
14
15 can still expect this to be a factor affecting assay precision in the detection of real
16
17 samples.
18
19
20
21
22
23
24
25
26

27 **4. Conclusions**

28
29 We have described a highly sensitive method of detecting DNA hybridisation based
30
31 on mediated electron transfer from a redox-labeled stem loop probe. The redox label
32
33 consisted of a PSA sphere loaded with a high quantity of MB. Two issues arose from
34
35 the use of this label: 1) Whether steric hindrance from neighbouring probes would
36
37 prevent adequate label - electrode contact. 2) Whether charge from all the MB on the
38
39 PSA sphere would be able to precolate to the electrode. To avoid these problems we
40
41 employed the $\text{Fe}(\text{CN})_6^{3-/4-}$ redox couple in solution, to mediate charge transfer from
42
43 the MB label. This relatively simple strategy enabled us to lower the LOD of the
44
45 assay by three orders of magnitude, relative to direct MB reduction. To the best of
46
47 our knowledge, this is the lowest reported DNA detection limit achieved by a redox
48
49 label in the absence of an enzyme. Issues remaining with this method are the fact that
50
51 a number of preparative steps are required before the analytical signal can be realised.
52
53 These include the solution-phase hybridisation reaction, confinement of the stem loop
54
55
56
57
58
59
60

1
2
3 to the electrode surface and attachment of the MB ball label. The number of
4
5 experimental steps are reflected in the error bars we reported for both calibrations.
6
7 Therefore, further work should include the development of strategies which provide
8
9 adequate detection limits while requiring less experimental steps. This will be very
10
11 challenging. There may have to be a compromise between method simplicity and
12
13 sensitivity.
14
15
16
17
18
19
20
21
22
23
24

25 **Acknowledgements**

26
27 U. N. acknowledges a PhD scholarship from the Royal Golden Jubilee Project of the
28
29 Thailand Research Fund, in cooperation with King Mongkut's University of
30
31 Technology Thonburi (PHD/0318/2550). This project received financial support from
32
33 the National Research University Project of Thailand's Office of Higher Education
34
35
36
37
38
39
40
41
42
43
44
45
46
47
48
49
50
51
52
53
54
55
56
57
58
59
60
60

References

- 1 L. Niessen, J. Luo, C. Denschlag and R. F. Vogel, *Food Microb.*, 2013, **36**, 191.
- 2 C. Green, J. F. Huggett, E. Talbot, P. Mwaba, K. Reither, and A. I Zumla, *Lancet Infect. Dis.* 2009, **9**, 505.
- 3 S.-M. Ho and W.-Y. Tang, *Rep. Toxicol.*, 2007, **23**, 267.
- 4 P. Pandeshwar and R. Das, *J. Forensic Legal Med.*, 2014, **22**, 45.
- 5 S. Tombelli, M. Minunni and M. Mascini, *Biomol. Eng.*, 2007, **24**, 191.
- 6 C. Zhang, J. Xu, W. Ma, W. Zheng, *Biotechnol. Adv.*, 2006, **24**, 243.
- 7 X. Hun, H. C. Chen and W. Wang, *Biosens. Bioelectron.*, 2010, **26**, 248.
- 8 D. Wu, B. C. Yin and B. C. Ye, *Biosens. Bioelectron.*, 2011, **28**, 232.
- 9 D. Thipmanee, S. Samanman, S. Sankoh, A. Numnuam, W. Limbit, P. Kanatharana, T. Vilaivan and P. Thavarungkul, *Biosens. Bioelectron.*, 2012, **38**, 430.
- 10 S. Samanman, P. Kanatharana, P. Aswatreratanakul and P. Thavarungkul, *Electrochim. Acta*, 2012, **80**, 202.
- 11 F. Lucarelli, G. Marrazza, A. P. F. Turner and M. Mascini, *Biosens. Bioelectron.*, 2004, **19**, 515.
- 12 J. Wang, G. Liu and M. Jan, *J. Am. Chem. Soc.*, 2004, **126**, 3010.
- 13 I. Willner and E. Katz, *Angew. Chem. Int. Ed.*, 2004, **43**, 6042.
- 14 Y. Ding, Q. Wang and F. Gao, *Electrochim. Acta*, 2013, **106**, 35.
- 15 Z. W. Chen, A. Balamurugan and S-M. Chen, *Bioelectrochem.*, 2009, **75**, 13.
- 16 L. E. Ahangar and M. A. Mehrgardi, *Biosens. Bioelectron.*, 2012, **38**, 252.
- 17 R. Garcia-Gonzalez, A. Costa-Garcia and M. T. Fernandez-Abedul, *Sens. Act. B*, 2014, **191**, 784.

- 1
2
3 18 G. Chatelain, M. Ripert, C. Farre, S. A. Alex and C. Chaix, *Electrochim. Acta*,
4 2012, **59**, 57.
5
6
7 19 W. C. Liao and J.-A. Ho, *Anal. Chem.*, 2009, **81**, 2470.
8
9
10 20 Y. Li, H. Qi, F. Fang and C. Zhang, *Talanta*, 2007, **72**, 1704.
11
12 21. S. Pinijsuwan, P. Riviravanich, M. Somasundrum and W. Surareungchai,
13 *Anal. Chem.*, 2008, **80**, 6779.
14
15
16 22 T. Li, K. Aoki, J. Chen and T. Nishiumi, *J. Electroanal. Chem.*, 2009, **633**,
17 319.
18
19
20 23 Y. Nagooka, S. Shiratori and Y. Einaga, *Chem. Mater.*, 2008, **20**, 4004.
21
22
23 24 Y. Zhou and Y. Li, *Langmuir*, 2004, **20**, 7208.
24
25 25 P. Rijiravanich, K. Aoki, J. Chen, W. Surareungchai and M. Somasundrum,
26 *Electroanalysis*, 2004, **16**, 605.
27
28
29 26 www.rnasoft.ca/cgi-bin/RNAsoft/Pairfold/pairfold.pl
30
31
32 27 S. S. Ivanov, A. S. Chung, Z.-I. Yuan, Y.-I. Guan, K. V. Sachs, J. S. Reichner
33 and Y. E. Chin, *Mol. Cell. Proteom.*, 2004, **3**, 788.
34
35
36 28 S. Wildsmith and F. Spence, in *An Introduction to Toxicogenomics*, M. E.
37 Burczynski, (Ed.) 2003. CRC Press, Boca Raton, USA, p 14.
38
39
40 29 J. Mocak, A. M. Bond, S. Mitchell and G. Scollary, *Pure & Appl. Chem.*,
41 1997, **69**, 297.
42
43
44 30 V. Ostanta, D. Dolinnaya, S. Andreev, T. Oretskaya, J. Wang and T. Hianik,
45 *Bioelectrochem.*, 2005, **67**, 205.
46
47
48 31 Chunglok, W., Khownarumit, P., Rijiravanich, R., Somasundrum, M.,
49 Surareungchai, W., 2011. *Analyst* **136**, 2969-2974.
50
51
52 32 E. E. Ferapontova, M. N. Hansen, A. M. Saunders, S. Shipovskov, D. S.
53 Sutherland and K. V. Gothelf, *Chem. Comm.*, 2010, 1836.
54
55
56
57
58
59
60

1
2
3 33 L. Chen, L. Zhang, T. Qiu and W. Cao, *Int. J. Electrochem. Sci.*, 2011, **6**,
4 5325.
5
6

7 34 Y. He, Y. Chai, R. Yuan, H. Wang, L. Bai, Y. Cao and Y. Yuan, *Biosens.*
8 *Bioelectron.*, 2013, **50**, 294.
9
10
11
12
13
14
15
16
17
18
19
20
21
22
23
24
25
26
27
28
29
30
31
32
33
34
35
36
37
38
39
40
41
42
43
44
45
46
47
48
49
50
51
52
53
54
55
56
57
58
59
60

Legends For Figures

- 1
2
3
4
5
6
7
8
9
10
11
12
13
14
15
16
17
18
19
20
21
22
23
24
25
26
27
28
29
30
31
32
33
34
35
36
37
38
39
40
41
42
43
44
45
46
47
48
49
50
51
52
53
54
55
56
57
58
59
60
- Figure 1 UV spectra of PSA-(PAA/PSS)₂(MB/PSS)₃ spheres following dissolution in THF (A), and a solution of 2 μ M MB dissolved in MilliQ water (B).
- Figure 2 Ratio of DPV peak heights in the absence (I_0) and presence (I) of 1 pM target DNA, shown as a function of anti-DIG concentration applied to the poly-L-lysine modified screen printed electrode. Error bars show \pm 1 std. dev. ($n = 5$).
- Figure 3 Response to target DNA as a function of hybridisation temperature using screen printed electrodes modified by a 19.9 μ g mL⁻¹ anti-DIG solution. I_0 and I are as defined in Fig. 1. Error bars show \pm 1 std. dev. ($n = 5$).
- Figure 4 Background-subtracted DPV peak current from MB reduction to different target sequences. The background value is taken as the response to buffer.
- Figure 5 Calibration of 30 mer DNA target based on the DPV peak height from the direct reduction of MB. Error bars show \pm 1 std. dev. ($n = 5$). Inset: Examples of DPVs recorded using 1 pM (\square), 100 fM (\blacksquare), 25 fM (\blacktriangledown), 10 fM (Δ), 2.5 fM (\circ), and 1.0 fM (\bullet) of target.

1
2
3
4
5 Figure 6 DPV of 1.0 pM target following hybridisation procedure in the absence
6
7 (●) and presence (○) of 0.25 mM $\text{Fe}(\text{CN})_6^{3-}$. Inset: I/I_0 ratio as defined
8
9 in Fig. 1 shown as a function of $\text{Fe}(\text{CN})_6^{3-}$ concentration for the
10
11 cathodic peak for direct MB reduction (○) and $\text{Fe}(\text{CN})_6^{3-}$ -mediated
12
13 reduction (●).
14
15
16
17

18
19 Figure 7 Calibration of 30 mer DNA target by DPV in the presence of 0.25 mM
20
21 $\text{Fe}(\text{CN})_6^{3-}$ as a solution phase mediator. Error bars show ± 1 std. dev.
22
23 (n = 5).
24
25
26
27

28
29 Scheme 1 Schematic representation of the hybridisation assay using $\text{Fe}(\text{CN})_6^{3-}$
30
31 mediation. The stem loop probes are attached to the surface of screen
32
33 printed electrodes by DIG tags binding to immobilised anti-DIG
34
35 antibodies. When hybridisation does not occur, steric hindrance
36
37 prevents the MB ball label from attaching to the stem loop.
38
39
40
41
42
43
44
45
46
47
48
49
50
51
52
53
54
55
56
57
58
59
60

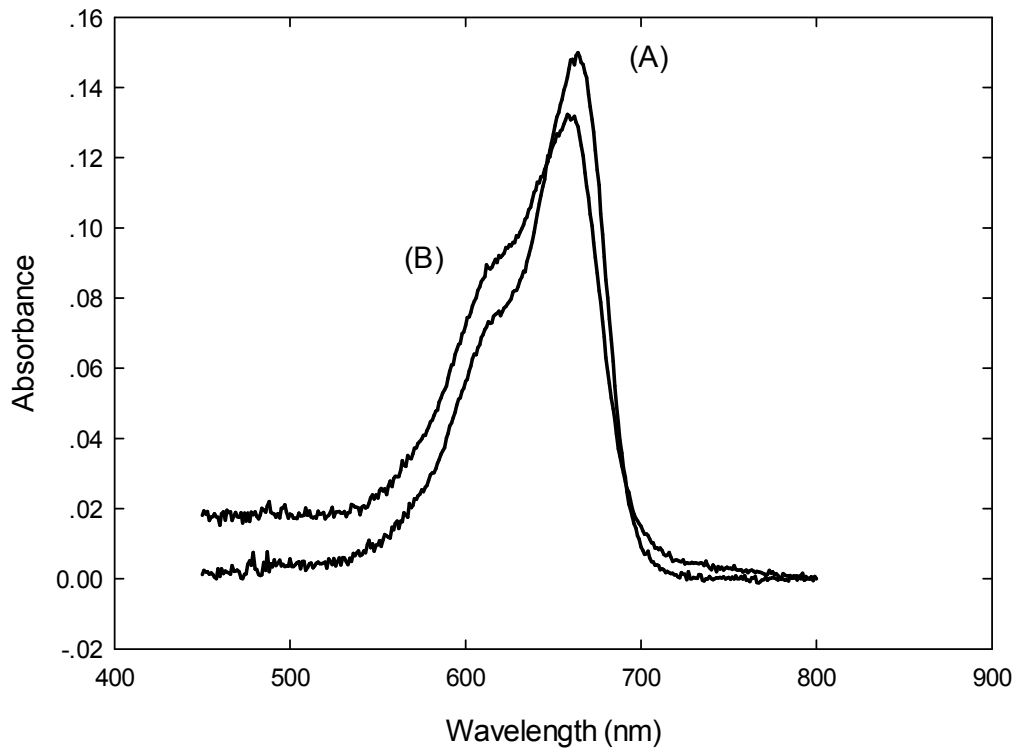


Figure 1

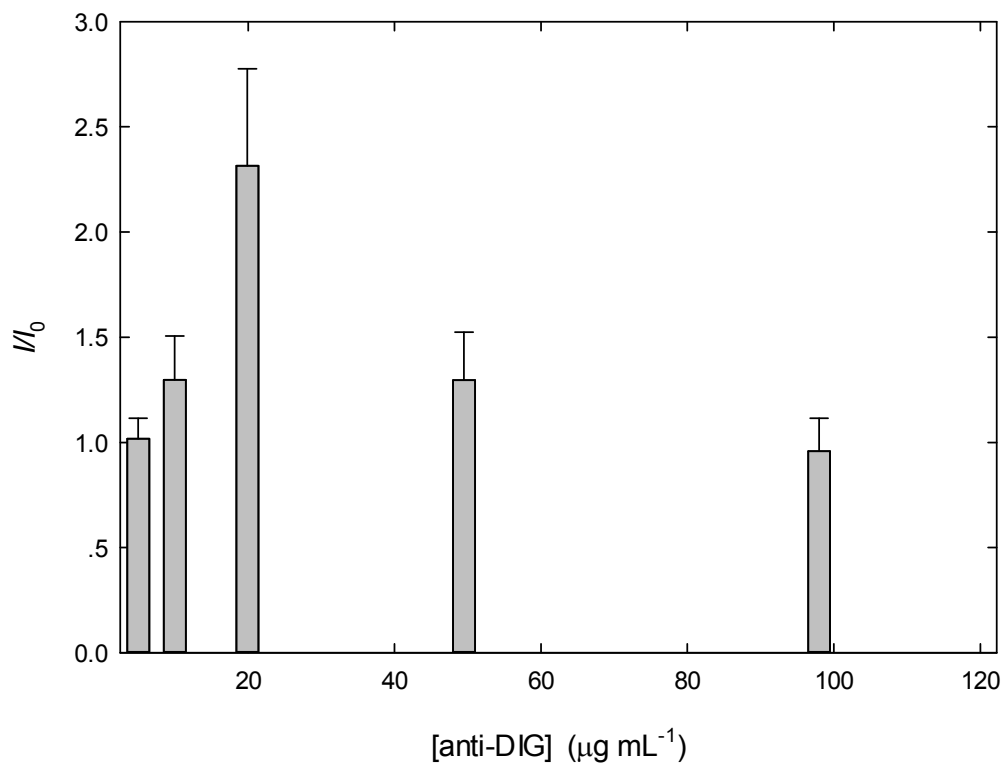


Figure 2

1
2
3
4
5
6
7
8
9
10
11
12
13
14
15
16
17
18
19
20
21
22
23
24
25
26
27
28
29
30
31
32
33
34
35
36
37
38
39
40
41
42
43
44
45
46
47
48
49
50
51
52
53
54
55
56
57
58
59
60

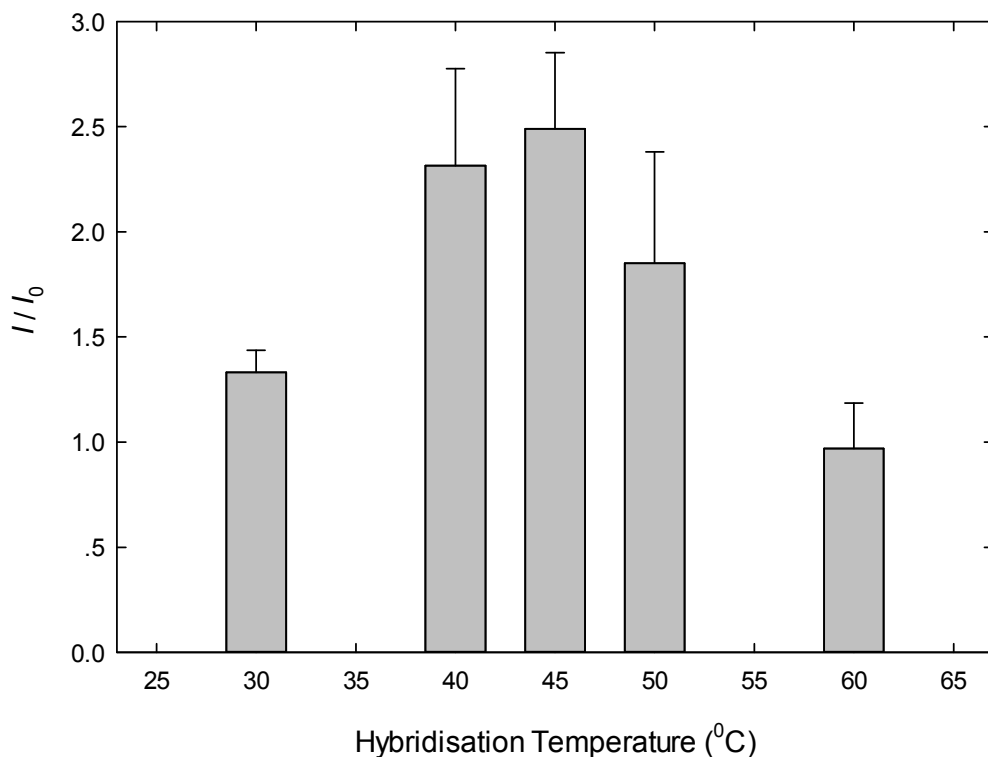


Figure 3

Analyst Accepted Manuscript

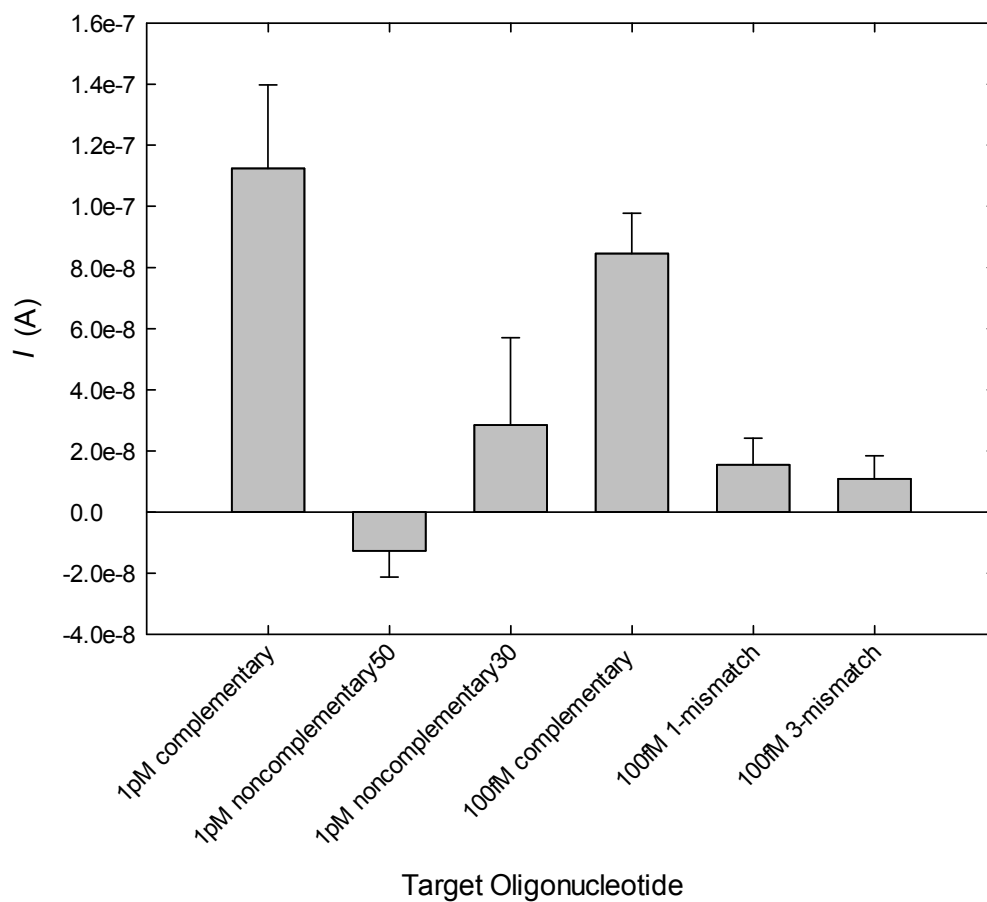


Figure 4

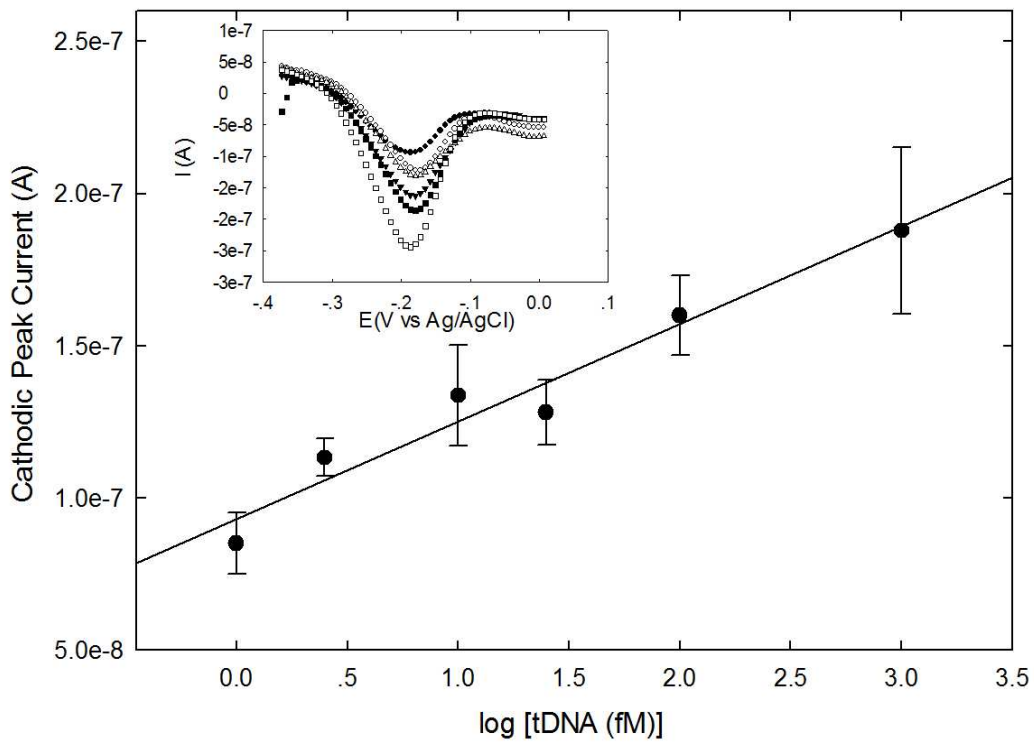


Figure 5

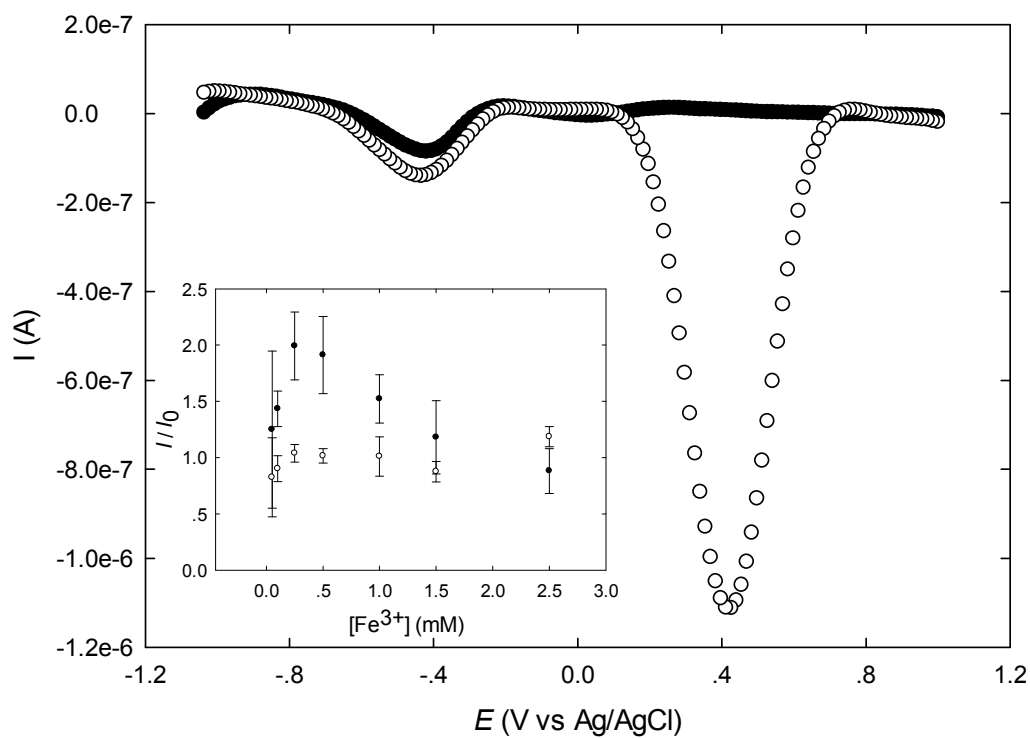


Figure 6

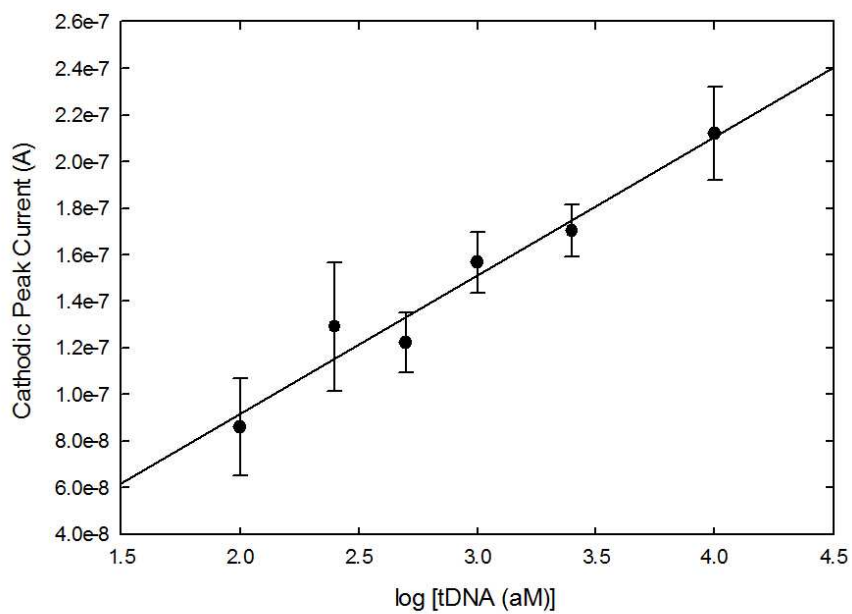
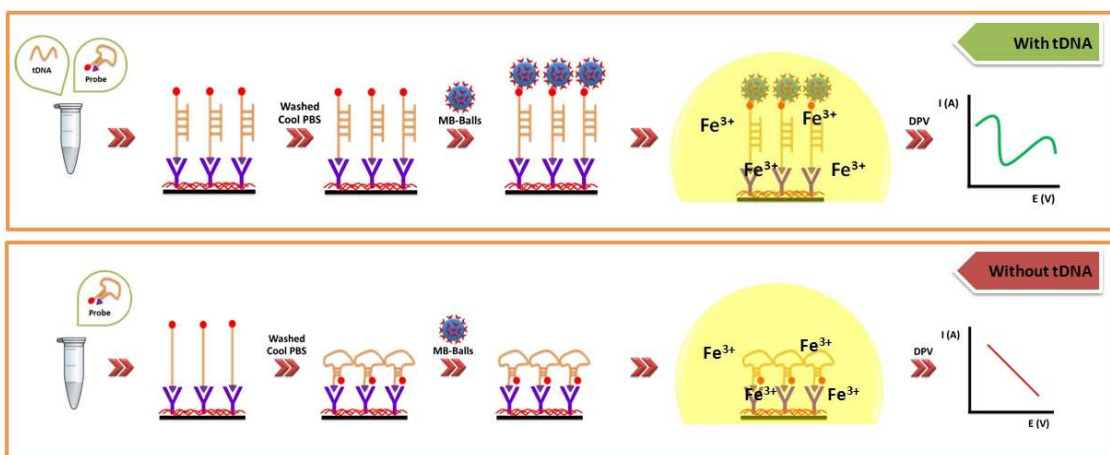


Figure 7



Scheme 1